Terrace and step contributions to the optical anisotropy of Si(001) surfaces

W. G. Schmidt* and F. Bechstedt
IFTO, Friedrich-Schiller-Universität, 07743 Jena, Max-Wien-Platz 1, Germany

J. Bernholc
Department of Physics, North Carolina State University, Raleigh, North Carolina 27695-8202
(Received 5 June 2000; published 9 January 2001)

The contributions of atomically flat terraces as well as of S_A, S_B, and D_B steps to the optical anisotropy of Si(001) surfaces have been calculated using a real-space multigrid method together with *ab initio* pseudopotentials. Our results for ideal (1×2), $p(2\times2)$, and $c(2\times4)$ reconstructed surfaces show a distinct influence of the dimer arrangement on the optical spectra. The calculated spectrum for the Si(001)$c(2\times4)$ surface agrees best with the signal measured for atomically smooth terraces. The significant optical anisotropy around 3 eV observed for vicinal surfaces, however, is induced by surface steps. Both electronic transitions directly at the surface as well as in deeper layers contribute to the optical anisotropy. We identify two mechanisms causing anisotropy signals from layers beneath the surface: the influence of the anisotropic surface potential on the bulk wave functions as well as minor contributions from atomic relaxations caused by surface-induced stress.

DOI: 10.1103/PhysRevB.63.045322 PACS number(s): 78.66.Db, 73.20.At, 71.15.Mb

I. INTRODUCTION

The optical spectroscopy of surfaces, in particular reflectance anisotropy spectroscopy or reflectance difference spectroscopy (RAS/RDS), is an extremely versatile tool of surface analysis.[1,2] Thanks to the development of both computational techniques and resources it is now possible to calculate anisotropy spectra from *first principles* in quantitative agreement with the measured data.[3–5] Such calculations are very involved, however, and have by now been restricted to ideal surfaces. Realistic surfaces, and growth structures in particular, however, are characterized by defects such as surface steps, which give rise to distinct optical anisotropies.[6–8] The theoretical description of these step-related optical anisotropies is therefore important in the context of the correct interpretation of RAS spectra measured during growth.

Apart from the assignment of structural features to optical fingerprints, which can be greatly assisted by calculations, there is also a more fundamental interest in an accurate theoretical description of RAS. While the contributions of transitions between electronic surface states to the anisotropy signal are now well understood,[3] there remain open questions concerning the origin of bulk-related features in the spectra (see, e.g., Ref. 9). A dynamic photon-induced localization of the initial and final states was suggested to account for anisotropy signals close to the bulk critical point (CP) energies.[10] Also the quenching of bulk-state wave functions near the surface was made responsible for such peaks.[11] Hingerl *et al.*[12] relate RAS features arising from bulk layers to inequivalent atomic displacements induced by anisotropic surface stress.

The optical anisotropy of the Si(001) surface has been intensively studied by both experiment[7,8,13–18] and theory,[18–23] due to its technological importance and its model character for semiconductor surface science. The understanding of the origins of particular features in the RAS of Si(001) is limited, however, in spite of these efforts. Two recent *ab initio* studies[21,22] arrive at different conclusions for the optical anisotropy of ideal Si(001) surfaces. The influence of surface steps on the optical anisotropy of Si(001) is unresolved. Some studies[16,18] suggest that steps play only a minor role for the optical anisotropy. Other authors[8,13] find a substantial step-induced contribution to the optical signal. Step contributions to the RAS may be related to the influence of the surface steps on the reconstruction of the terraces as assumed in Ref. 13, to the changed bonding configuration of the steps themselves, as hypothesized in Ref. 8, or to transitions between bulk wave functions, modified by surface steps, as recently found for Si(111):H surfaces.[24]

In the present study we clarify this issue using *first-principles* calculations of the surface optical anisotropy. Both the RAS of ideal, atomically flat Si(001) surfaces forming (1×2), $p(2\times2)$, and $c(2\times4)$ reconstructions and of defect structures, modeling S_A, S_B, and D_B steps are investigated. Particular attention is paid to the origin of bulk-related features in the optical spectra.

II. METHOD

The calculations have been carried out using the same method as in our recent studies on the optical properties of vicinal Si(111):H surfaces and III-V(001) growth planes.[24–26] In short, we use density-functional theory in the local-density approximation (DFT-LDA) together with nonlocal norm-conserving pseudopotentials[27] to determine the structurally relaxed ground state of the system. A massively parallel, real-space finite-difference method[28] is used to deal efficiently with the large surface unit cell and the many states required for the calculation of the dielectric function. A multigrid technique is employed for convergence acceleration. The spacing of the finest grid used to represent the electronic wave functions and charge density was determined through a series of bulk calculations. We find that structural and electronic properties are converged for a spacing of 0.238 Å.

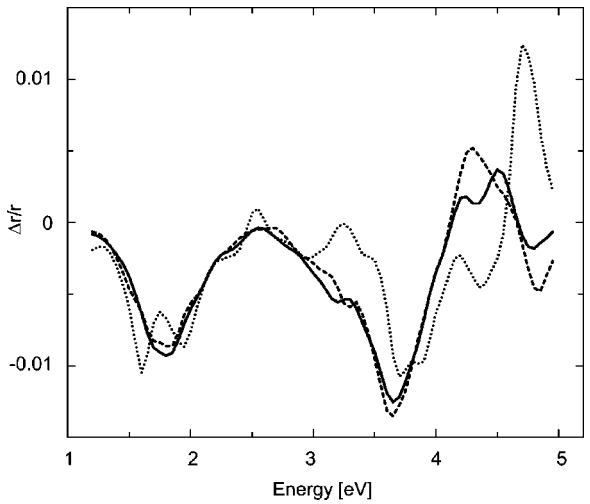

FIG. 1. RAS spectra $[\mathrm{Re}\{(r_{[1\bar{1}0]}-r_{[110]})/\langle r\rangle\}]$ calculated for the Si(001)$c(2\times4)$ surface using uniform meshes of **k** points corresponding to 64 (dotted line), 256 (dashed line), and 1024 (solid line) points in the full (1×1) surface Brillouin zone.

This corresponds to an energy cutoff in plane-wave calculations of about 24 Ry. The calculations yield a bulk equilibrium lattice constant of $a_{eq}=5.378$ Å and a bulk modulus of $B=0.979$ Mbar (experiment:[29] 5.43 Å and 0.96–0.99 Mbar). The calculated excitation energies suffer from the neglect of self-energy effects in DFT-LDA and are smaller than the measured values: The calculated indirect band gap is 0.58 eV (room-temperature experiment:[29] 1.11 eV). A similar underestimation of about 0.5 eV occurs for the E_1 and E_2 critical points (CP's) of the bulk band structure, for which we obtain 3.0 and 3.8 eV, respectively. In order to compare the theoretical spectra with experiment we apply an upward rigid shift of 0.5 eV to the conduction bands and renormalize the momentum matrix elements accordingly.[30] The results are in agreement with *GW* calculations on Si surfaces.[31,32] The slab polarizability calculated in the independent-particle approximation is used to calculate the RAS spectra.[33,34] Our study is thus on the same level as other recent *ab initio* studies of the optical properties of Si surfaces.[18,22,24]

To model the step configurations we consider periodic supercells along the surface normal. They contain asymmetric slabs, consisting of 11 atomic Si layers, separated by 12 Å of vacuum. The dangling bonds at the bottom layer are saturated with hydrogen. The investigated geometries were carefully relaxed until all calculated forces were below 10 meV/Å. The atoms in the lowest two atomic layers were kept frozen in the ideal bulk configuration. Integrations in the surface Brillouin zone (SBZ) for calculating the atomic and electronic ground state of the system were performed using two special **k** points in the irreducible part.

The **k**-space sampling in calculating the dielectric function is of central importance for the quality of the surface optical spectra.[35] Figure 1 shows the RAS calculated for Si(001)$c(2\times4)$ using uniformly distributed **k** points corresponding to densities of 64, 256, and 1024 points in the full (1×1) SBZ. The figure shows that in particular the high-energy features are not completely converged using the 256 **k**-point set. Therefore we used a sampling corresponding to 1024 points for the ideal surfaces, and 576 and 784 points, respectively, for the defect structures used to model S_A and S_B/D_B steps. All conduction bands within 9 eV of the top of the valence bands were included in the calculation of the dielectric function.

III. RESULTS AND DISCUSSION

A. Flat surface

Clean Si(001) surfaces reconstruct due to the dimerization of the topmost atoms. The dimers are asymmetric, consisting of an sp^2-like bonded ''down'' atom, which moves closer to the plane of its three nearest neighbors, and an ''up'' atom, which moves away from the plane of its neighbors and possesses an *s*-like dangling bond. When the dimers buckle in the same direction, the surface periodicity remains (1×2). If no pinning due to surface defects occurs, however, the direction of buckling alternates within each dimer row. This reduces the energy due to relaxation of local stress and, possibly, to improved electrostatics.[36] Depending on the registry of buckling in the neighboring dimer rows, this alternation leads to $p(2\times2)$ or $c(2\times4)$ periodicities. We calculate an energy gain of 56 meV per surface dimer for the transition from the (1×2) to a $p(2\times2)$ reconstruction. A further lowering of the surface energy by 7 meV per dimer occurs for the transition from the $p(2\times2)$ to a $c(2\times4)$ surface. These energy differences are in agreement with earlier studies (see, e.g., Ref. 37) and of the same order of magnitude as the thermal energy kT, at room temperature (25 meV). The symmetry of the dimer arrangement has some influence on the dimer geometry. Our calculations yield a buckling of 0.74, 0.76, and 0.80 Å, respectively, for dimers forming (1×2), $p(2\times2)$, and $c(2\times4)$ periodicities. These values are close to the ones obtained by Palummo *et al.*,[22] but are somewhat larger than calculated by Kipp and co-workers.[18]

The RAS spectra calculated for (1×2), $p(2\times2)$, and $c(2\times4)$ reconstructed Si(001) are shown in Fig. 2. The spectrum for (1×2) is characterized by a pronounced minimum at 1.4 eV, a rather broad negative anisotropy between 2.5 and 4.0 eV and a maximum at 4.5 eV. Our results are consistent with previous *ab initio* results.[18,22]

The alternating arrangement of the asymmetric dimers in a $p(2\times2)$ rather than a (1×2) structure leads to pronounced spectral changes. Two distinct minima appear, $T1$ at 1.7 eV and $T3$ at 3.6 eV, close to the E_1 CP. The strong influence of the dimer arrangement on the RAS is caused by the strong interdimer interactions at Si(001) surfaces. Compared to, e.g., C(001) surfaces, intradimer hopping is less important and the optical matrix elements are mostly determined by hopping through nearby dimers and subsurface orbitals, as discussed by Kress *et al.*[20] The dimer-dimer interaction extends even beyond the dimer rows: differences in the RAS also appear in the spectra calculated for $p(2\times2)$ and $c(2\times4)$ surfaces. $T1$ shifts from 1.7 to 1.8 eV and the local minimum at 2.4 eV (R in Fig. 2) evolves into a shoulder. A new feature, $T2$, appears at 3.2 eV. The strong influence of the dimer symmetry and arrangement on the RAS

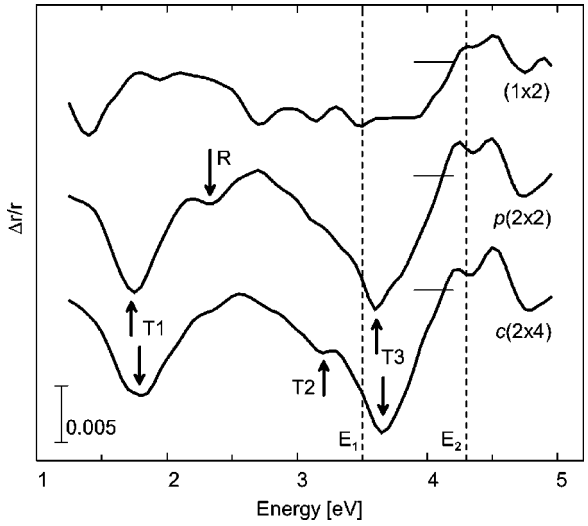

FIG. 2. RAS spectra $[\mathrm{Re}\{(r_{[1\bar{1}0]}-r_{[110]})/\langle r\rangle\}]$ calculated for the Si(001)(1×2), $p(2\times2)$, and $c(2\times4)$ surfaces. Dashed lines mark the positions of bulk critical point energies.

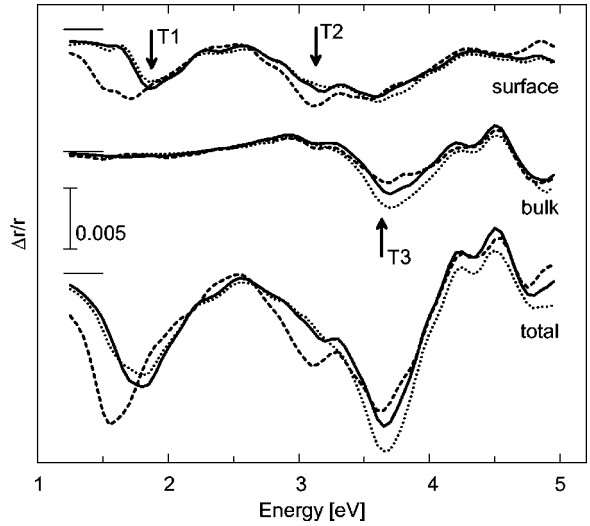

FIG. 4. RAS for the Si(001)$c(2\times4)$ surface, calculated for the fully relaxed configuration (solid lines) in comparison to calculations for a geometry where the relaxation was restricted to the uppermost two atomic layers (dashed lines). Spectra calculated for an anisotropically strained slab (see text) are shown by dotted lines. Shown are contributions to the RAS from electronic transitions within the uppermost four atomic layers, from the layers underneath, and the total signal.

spectra of Si(001) suggests to clarify the assumed low-temperature phase transition of this surface[38] by means of optical spectroscopy.

In order to determine the local origin of the spectral features we used a linear cutoff function to separate the contributions to the RAS from electronic transitions within the uppermost four atomic layers and from the bulklike layers underneath. Figure 3 shows that surface-state related transitions are mainly responsible for the optical anisotropies below the E_1 CP energy. This holds in particular for the features R, $T1$, and $T2$. In bulk Si there are no direct transitions below 3.4 eV, therefore no bulk-state contributions to the RAS appear for low energies. Surface modified bulk wave functions are mainly responsible for $T3$ and two maxima below and above the E_2 CP energy. These maxima depend only little on the surface symmetry and appear for (1×2), $p(2\times2)$, and $c(2\times4)$ periodicities.

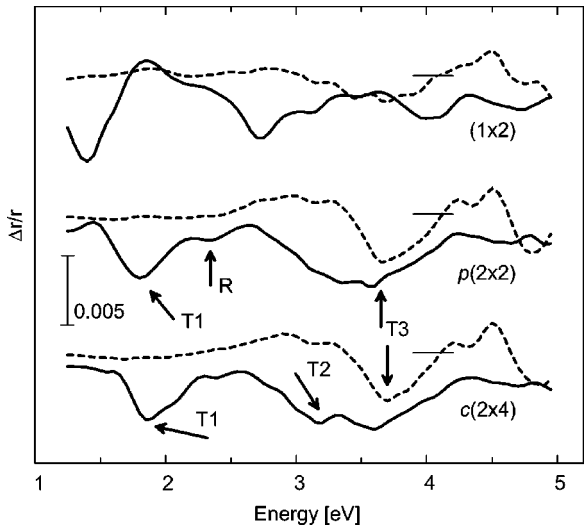

FIG. 3. Surface (solid lines) and bulk contributions (dashed lines) to the calculated RAS for the Si(001)(1×2), $p(2\times2)$, and $c(2\times4)$ surfaces (see text).

The appearance of optical anisotropies which are *not* related to transitions between surface states has led to controversial discussions. Recently, it has been suggested that subsurface stress due to the dimerization of the surface atoms may be largely responsible for RAS contributions from deeper layers.[12] We performed additional calculations in order to investigate the influence of surface stress on the optical spectra. First, we study a Si(001)$c(2\times4)$ geometry where only the uppermost two atomic layers were allowed to relax, and the remaining atoms occupy their ideal bulk positions. Such an artificial structure is higher in energy by 221 meV per dimer compared to the fully relaxed configuration. The dimer buckling is reduced by 0.04 Å. Figure 4 shows the RAS spectrum of the configuration with surface-restricted relaxation (dashed lines) in comparison with the results for the fully relaxed geometry (solid lines). The surface-related RAS minimum $T1$ becomes more pronounced and shifts to 1.6 eV. The restriction of the relaxation leads, furthermore, to a modification of the $T2$ and $T3$ features. Small modifications occur also for the RAS arising from electronic transitions below the uppermost four atomic layers.

A second possibility to probe the influence of surface stress on the optical spectra consists of slightly changing the lateral dimensions of the surface unit cell. The dimerized surface feels stretched along the dimer bonds and compressed across the dimer rows.[36] Accordingly, we relax the Si(001)$c(2\times4)$ surface in a unit cell whose lateral dimensions are shrunk/enlarged by 0.5 % along $[110]/[\bar{1}10]$. The RAS spectra calculated for this configuration are shown by dotted lines in Fig. 4. The optical anisotropies arising from

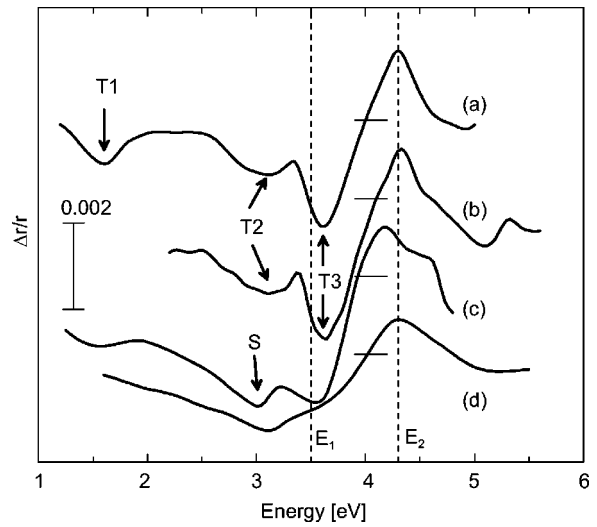

FIG. 5. RAS spectra $[\mathrm{Re}\{(r_{[1\bar{1}0]}-r_{[110]})/\langle r\rangle\}]$ measured for the clean Si(001) surfaces. The data (a), (b), (c), and (d) are taken from Refs. 13, 8, 18, and 15, respectively. Dashed lines mark the positions of bulk critical point energies.

subsurface transitions are slightly affected. In particular the $T3$ feature is enhanced. It may thus be partially attributed to reconstruction-induced stress in the layers beneath the surface. Our results show that both the structural relaxation in the bulk and anisotropic strain fields modify the bulk-related optical anisotropy. Its salient features, however, are not affected. This indicates that, at least in the case studied here, the anisotropic surface potential induces optical anisotropies in the bulk via a pure electronic coupling.

The comparison of the calculated spectra with experimental data is not straightforward. On the one hand, due to the size of the systems studied here, excitonic effects[39] are completely neglected. Self-energy corrections of the optical spectra[3,4] are crudely approximated by a scissors operator. Some error cancellation may be expected, though, since RAS spectra are difference spectra, and, furthermore, normalized to the bulk dielectric function. On the other hand, there are experimental limitations. The magnitude of the measured reflectance anisotropy[8,13,15,18] is only about half as large as the calculated signal. That may be related to some cancellation of anisotropy signals from (1×2) and (2×1) domains in the experiments. Temperature effects and sample imperfections neglected in our calculation also reduce the measured anisotropy signal. Additionally, the experimental spectra are clearly dependent on the surface preparation. This is obvious from Fig. 5, where we compiled data measured by four different groups for clean Si(001) surfaces. Shioda and van der Weide[13] obtained their data from a highly oriented surface, prepared by an electromigration technique, resulting in large terraces covered with uniformly oriented dimers. Jaloviar *et al.*[8] prepared highly oriented Si(001) samples using a straining method, which also resulted in a low step density combined with a high population asymmetry between the (2×1) and (1×2) terraces. Kipp *et al.*,[18] as well as Yasuda and co-workers,[15] on the other hand, realized the population asymmetry between the (2×1) and (1×2) terraces on the Si(001) surface by using 4° vicinal samples.

All experimental spectra show common features, such as a maximum at or close to the E_2 CP energy and negative anisotropies around the E_1 energy. However, there are also differences. The spectra obtained from vicinal samples have a minimum around 3 eV (denoted S in Fig. 5). Since hydrogen exposure influences line shape and energetic position of that feature, Mantese and co-workers[7] concluded that S is related to dimer dangling bonds. Such an interpretation does not explain, however, why the feature does not appear in the spectra measured for highly oriented samples.[8,13] The latter, instead, are characterized by minima at 1.6, 3.1, and 3.6 eV ($T1$, $T2$, and $T3$ in Fig. 5).

Comparing the RAS calculated for (1×2), $p(2\times2)$, and $c(2\times4)$ reconstructed surfaces in Fig. 2 with the experimental curves (a) and (b) in Fig. 5, we find that the calculated anisotropy for $c(2\times4)$ surfaces agrees best with the anisotropy measured for highly oriented samples. The experimental features $T1-3$ are reproduced. The agreement is not perfect, however. The calculations yield two maxima at 4.2 and 4.5 eV, rather than the single maximum close to the E_1 energy observed experimentally. Figure 1 shows that this splitting occurs only for calculations with a high **k**-point density. Such a splitting may be observable at low temperatures, as recently demonstrated for InP(001) surfaces.[3] The experiments on Si(001) were performed at room temperature. We cannot exclude, however, that it is simply an artifact of our theoretical and computational limitations.

The spectrum calculated for $p(2\times2)$ surfaces fits the experimental curves (a) and (b) in Fig. 5 somewhat worse than the $c(2\times4)$ results. It shows a minimum at 2.4 eV (R in Fig. 2) which is not observed experimentally. The calculations for $p(2\times2)$ also fail to reproduce the measured $T2$ feature.

In Ref. 13 it was argued that surface steps on vicinal surfaces suppress the formation of surface reconstructions larger than (1×2) and are thus responsible for the spectral differences between highly oriented and miscut samples. Indeed, steps on Si(001) act as pinning centers for the dimer buckling and thus influence the surface reconstruction.[36] The agreement between the experimental data for vicinal samples, curves (c) and (d) in Fig. 5, and calculations for (1×2) periodicities is poor, however. If the (1×2) symmetry were stabilized versus larger reconstructions by surface steps, the spectrum calculated for (1×2) surfaces should show features characteristic for vicinal surfaces, such as the minimum S at 3 eV. This is not the case, however. Therefore it seems likely that surface steps are directly responsible for S, rather than via their influence on the terrace reconstruction.

B. Surface steps

According to the nomenclature introduced by Chadi,[40] Si(001) steps are classified into monatomic ''S'' (single) steps and biatomic ''D'' (double) steps. Both types are subdivided into A and B classes, depending on whether the dimers on the upper terrace are perpendicular or parallel to the step edge. Monoatomic steps separate (1×2) and (2×1) domains of dimerization, therefore S_A and S_B steps alternate. S_A steps do not require the formation of new or the

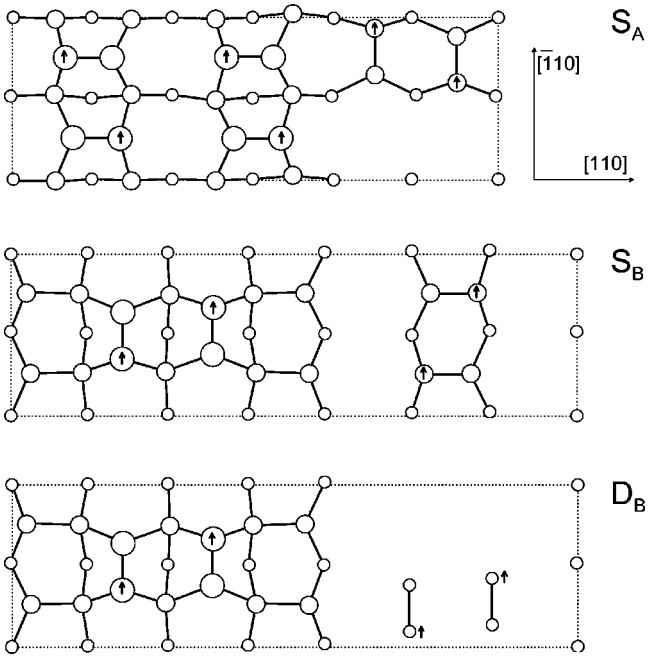

FIG. 6. Top view of dimer-vacancy structures used to model S_A, S_B, and D_B surface steps of Si(001). The size of the circles indicates their height. Arrows indicate dimer ''up'' atoms. Dotted lines mark the in-plane periodicity used in the calculation.

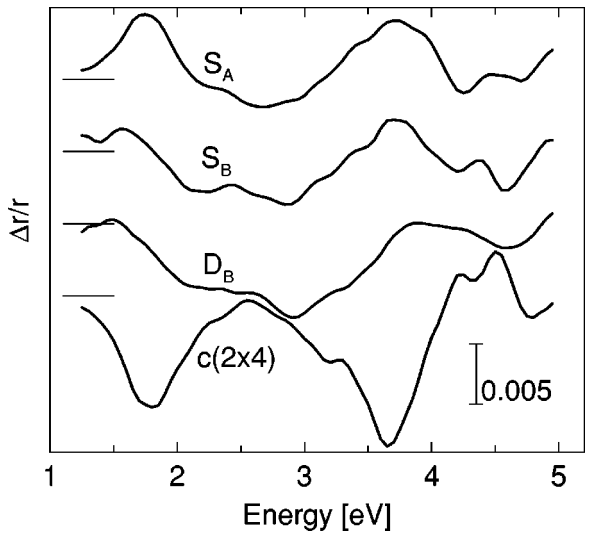

FIG. 7. RAS spectra $[\mathrm{Re}\{(r_{[\bar{1}10]}-r_{[110]})/\langle r\rangle\}]$ calculated for the dimer-vacancy structures shown in Fig. 6. For comparison also the spectrum calculated for the flat Si(001)$c(2\times4)$ surface is shown.

breaking of existing bonds. S_B steps, however, are more complicated and exist in three variations. All three types are observed in scanning tunneling microscopy, even though the rebonded version has the lowest formation energy.[36] The commonly observed biatomic steps are of type B and rebonded. The step height depends on the temperature and misorientation. Surface steps have monatomic height below a miscut angle θ of $1-2°$. For larger miscuts more and more biatomic steps are observed. The steps are almost exclusively biatomic for θ exceeding $6-8°$.[36]

In the present study we focus on the three most commonly observed step configurations: S_A steps and rebonded steps of type S_B and D_B. Since S_A and S_B steps cannot be separated on tilted surfaces, we model the steps as dimer-vacancy structures on ''flat'' surfaces, where they alternately raise and lower the terrace height. Figure 6 shows the considered defect structures. All possible symmetries for the arrangement of buckled dimers in the given surface periodicities were probed. The relaxed geometries shown in Fig. 6 correspond to the lowest-energy configurations. For reasons of computer capacity we restrict ourselves to high step densities. Typical experimental step separations are obviously larger than what can presently be modeled in *ab initio* calculations. Assuming double-layer steps, the step separation for a miscut angle θ of 6° is about twice as large as the distance modeled here. The relaxation of step-induced surface stress extends more than 40 atomic layers into the bulk material,[41] much deeper than the 11 layers considered in our study. In Ref. 8 it was noted, however, that the step-induced anisotropy signal for Si(001) depends nearly linearly on the step density. A similar dependence was earlier obtained for Si(111): H vicinally cut toward $[11\bar{2}]$.[6] This indicates that the geometric details of the surface steps as well as their interaction are of minor importance for the optical anisotropy. Therefore, it can be expected that our calculations can be extrapolated to allow for a meaningful comparison with the measured data, simply by scaling the RAS intensity with the step density.

Figure 7 shows the RAS spectra calculated for the three defect structures used to model S_A, S_B, and D_B steps. Despite the different geometries, all three structures give rise to rather similar spectra, characterized by a broad negative anisotropy between 2 and 3.5 eV. Separating the contributions to the RAS from transitions between surface- and bulk-localized wave functions, we find that both contribute to that particular line shape. That is demonstrated for the S_A step in Fig. 8. Also shown are calculations for the same defect structure, but allowing only the uppermost three layers to relax. The relaxation of the deeper layers influences the bulk-related anisotropies slightly for energies above the E_1 CP. The overall dependence of the RAS signal on the stress relaxation is weak, however. That posteriorly justifies our attempt to calculate step-induced optical anisotropies with atomic slabs containing only 11 atomic layers.

The spectra calculated for the defect structures of Fig. 6 cannot immediately be compared with experiment, as the contributions from the upper and lower ''terraces'' do not cancel in case of the S_A and D_B steps. We use the results obtained for flat Si(001) surface to account for the uneven size distributions of lower and upper terraces. The corrected spectra are then divided by two, since there are two ''steps'' contained in each defect structure. In such a way we obtain the actual step-generated RAS signal, which is compared with the experimental findings[8] in Fig. 9. Given the limitations of our study discussed above, the comparison is gratifying. In agreement with experiment we find that surface steps on Si(001) give rise to a broad negative anisotropy below the E_1 CP energy, with a minimum at around 3 eV.

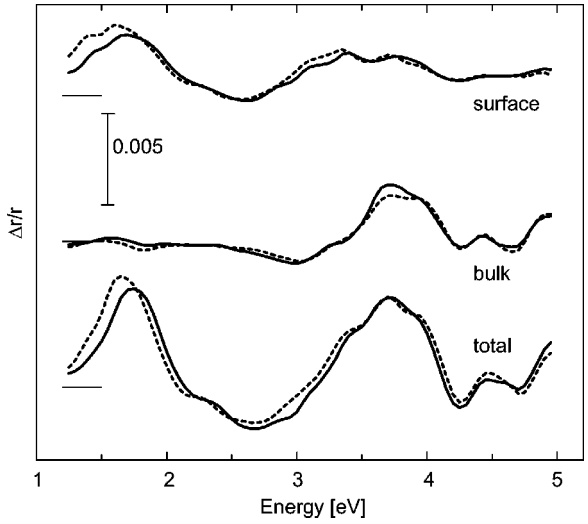

FIG. 8. RAS for the dimer vacancy structure used to model the S_A step, calculated for both the fully relaxed configuration (solid lines) and for a geometry where the relaxation was restricted to the uppermost three atomic layers (dashed lines). Shown are contributions to the RAS from electronic transitions within the uppermost four atomic layers, from the layers underneath, and the total signal.

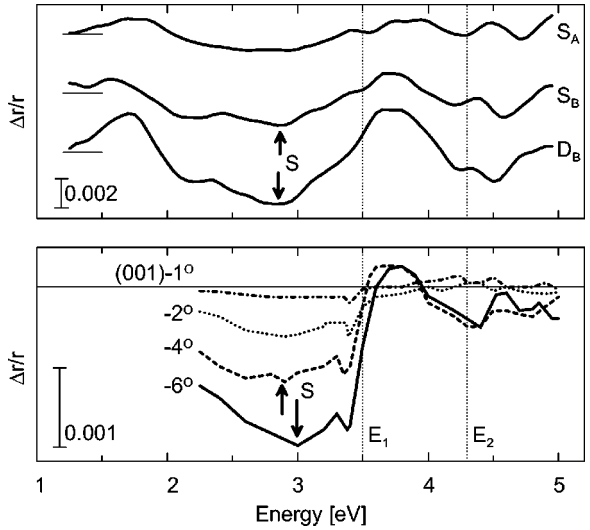

FIG. 9. Upper panel: Step-induced optical anisotropy $[\mathrm{Re}\{(r_{[1\bar{1}0]}-r_{[110]})/\langle r\rangle\}]$ calculated for S_A, S_B, and D_B steps. Lower panel: Step-induced optical anisotropy measured for different miscut angles as given in Ref. 8. Theoretical and experimental data refer to steps only. Terrace contributions have been subtracted (see text).

Experimentally a positive anisotropy between 3.5 and 4 eV is observed for miscut angles larger than 4°. A similar feature appears in the calculation for D_B steps. As biatomic steps form for larger miscuts only, the observed changes of the measured line shape with vicinality finds a natural explanation. The calculations do not explain, though, the sharp feature at 3.4 eV observed in Ref. 8. The procedure of subtracting the terrace contribution from the overall anisotropy, which was used to isolate the step-generated RAS in Ref. 8, is not really well defined, however. We speculate that the feature at 3.4 eV is an artifact of the local minimum between the terrace features $T2$ and $T3$ (cf. Figs. 2 and 5), rather than related to surface steps.

IV. SUMMARY

We presented a comprehensive *ab initio* study of the optical anisotropy of clean Si(001) surfaces. Flat (1×2), $p(2\times2)$, and $c(2\times4)$ reconstructed surfaces as well as defect structures modeling S_A, S_B, and D_B steps were considered. Our results for flat surfaces agree well with experiments performed on highly oriented samples. A remarkably large influence of the dimer symmetry on the RAS is found. The measured data can be best explained by the calculations for $c(2\times4)$ reconstructed surfaces. Electronic transitions both directly at the surface as well as from bulk layers contribute to the signal. The latter contributions are somewhat related to the relaxation of surface-induced stress but are mainly caused by the influence of the anisotropic surface potential on the bulk wave functions. Step contributions to the RAS have to be taken into account in order to understand data measured for vicinal surfaces. Both monatomic and biatomic steps generate a broad RAS feature at 3 eV. We find that the optical anisotropy induced by rebonded D_B steps is somewhat larger than the one caused by single layer steps of type S_A or S_B, in particular above the E_1 energy.

ACKNOWLEDGMENTS

We are indebted to D.E. Aspnes, K. Hingerl, and U. Rossow for suggesting this work and numerous useful discussions. Grants of computer time from the John von Neumann–Institut Jülich, the Konrad-Zuse-Zentrum Berlin and the DOD Challenge Program are gratefully acknowledged. J.B. was supported in part by ONR and the DOE.

*Email: W.G.Schmidt@ifto.physik.uni-jena.de

[1] D.E. Aspnes, Surf. Sci. **309**, 1017 (1994).
[2] W. Richter and J.T. Zettler, Appl. Surf. Sci. **101**, 465 (1996).
[3] W.G. Schmidt, N. Esser, A.M. Frisch, P. Vogt, J. Bernholc, F. Bechstedt, M. Zorn, T. Hannappel, S. Visbeck, F. Willig, and W. Richter, Phys. Rev. B **61**, R16 335 (2000).
[4] W.G. Schmidt, J.L. Fattebert, J. Bernholc, and F. Bechstedt, Surf. Rev. Lett. **6**, 1159 (1999).
[5] W. Lu, W. G. Schmidt, E. L. Briggs, and J. Bernholc, Phys. Rev. Lett. **85**, 4381 (2000).
[6] T. Yasuda, D.E. Aspnes, D.R. Lee, C.H. Bjorkman, and G. Lucovsky, J. Vac. Sci. Technol. A **12**, 1152 (1994).
[7] L. Mantese, U. Rossow, and D.E. Aspnes, Appl. Surf. Sci. **107**, 35 (1996).
[8] S.G. Jaloviar, J.-L. Lin, F. Liu, V. Zielasek, L. McCaughan, and M.G. Lagally, Phys. Rev. Lett. **82**, 791 (1999).
[9] R. Del Sole and G. Onida, Phys. Rev. B **60**, 5523 (1999).
[10] L. Mantese, K.A. Bell, D.E. Aspnes, and U. Rossow, Phys. Lett. A **253**, 93 (1999).
[11] K. Uwai and N. Kobayashi, Phys. Rev. Lett. **78**, 959 (1997).

[12] K. Hingerl, W. Hilber, R. E. Balderas-Navarro, A. Bonanni, and D. Stifter, Phys. Rev. B **62**, 13 048 (2000).
[13] R. Shioda and J. van der Weide, Phys. Rev. B **57**, R6823 (1998).
[14] R. Shioda and J. van der Weide, Appl. Surf. Sci. **130-132**, 266 (1998).
[15] T. Yasuda, L. Mantese, U. Rossow, and D.E. Aspnes, Phys. Rev. Lett. **74**, 3431 (1995).
[16] U. Rossow, L. Mantese, and D.E. Aspnes, J. Vac. Sci. Technol. B **14**, 3070 (1996).
[17] U. Rossow, L. Mantese, D.E. Aspnes, K.A. Bell, and M. Ebert, Phys. Status Solidi B **215**, 725 (1999).
[18] L. Kipp, D.K. Biegelsen, J.E. Northrup, L.-E. Swartz, and R.D. Bringans, Phys. Rev. Lett. **76**, 2810 (1996).
[19] A.I. Shkrebtii and R. Del Sole, Phys. Rev. Lett. **70**, 2645 (1993).
[20] C. Kress, A.I. Shkrebtii, and R. Del Sole, Surf. Sci. **377**, 398 (1997).
[21] V.I. Gavrilenko and F.H. Pollak, Phys. Rev. B **58**, 12 964 (1998).
[22] M. Palummo, G. Onida, R. Del Sole, and B.S. Mendoza, Phys. Rev. B **60**, 2522 (1999).
[23] N. Arzate and B. S. Mendoza (unpublished).
[24] W.G. Schmidt and J. Bernholc, Phys. Rev. B **61**, 7604 (2000).
[25] W.G. Schmidt, E.L. Briggs, J. Bernholc, and F. Bechstedt, Phys. Rev. B **59**, 2234 (1999).
[26] A.M. Frisch, W.G. Schmidt, J. Bernholc, M. Pristovsek, N. Esser, and W. Richter, Phys. Rev. B **60**, 2488 (1999).
[27] M. Fuchs and M. Scheffler, Comput. Phys. Commun. **119**, 67 (1999).
[28] E.L. Briggs, D.J. Sullivan, and J. Bernholc, Phys. Rev. B **54**, 14 362 (1996).
[29] *Semiconductors. Physics of Group IV Elements and III-V Compounds*, edited by K.-H. Hellwege and O. Madelung, Landolt-Börnstein, New Series (Springer-Verlag, Berlin, 1982), Group III, Vol. 17, Pt. a.
[30] R. Del Sole and R. Girlanda, Phys. Rev. B **48**, 11 789 (1993).
[31] J.E. Northrup, Phys. Rev. B **47**, 10 032 (1993).
[32] M. Rohlfing, P. Krüger, and J. Pollmann, Phys. Rev. B **52**, 1905 (1995).
[33] R. Del Sole, Solid State Commun. **37**, 537 (1981).
[34] F. Manghi, R. Del Sole, A. Selloni, and E. Molinari, Phys. Rev. B **41**, 9935 (1990).
[35] F. Bechstedt, O. Pulci, and W.G. Schmidt, Phys. Status Solidi A **175**, 5 (1999).
[36] J. Dabrowski and H.-J. Müssig, *Silicon Surfaces and Formation of Interfaces* (World Scientific, Singapore, 2000).
[37] P. Boguslawski, Q.-M. Zhang, Z. Zhang, and J. Bernholc, Phys. Rev. Lett. **72**, 3694 (1994).
[38] Y. Kondo, T. Amakusa, M. Iwatsuki, and H. Tokumoto, Surf. Sci. **453**, L318 (2000).
[39] S. Albrecht, L. Reining, R. Del Sole, and G. Onida, Phys. Rev. Lett. **80**, 4510 (1998).
[40] D.J. Chadi, Phys. Rev. Lett. **59**, 1691 (1987).
[41] T.W. Poon, S. Yip, P.S. Ho, and F.F. Abraham, Phys. Rev. Lett. **65**, 2161 (1990).